Femtosecond UV Excitation in Imidazolium-Based Ionic Liquids

N. Chandrasekhar, O. Schalk, and A.-N. Unterreiner*

Institut für Physikalische Chemie, Lehrstuhl für Molekulare Physikalische Chemie, Universität Karlsruhe (TH), D-76128 Karlsruhe, Germany

Received: June 2, 2008; Revised Manuscript Received: October 2, 2008

Femtosecond pump−probe absorption spectroscopy was employed to investigate ultrafast dynamics in various room temperature ionic liquids (RTILs) based on imidazolium cations, i.e., 1,3-dimethylimidazolium iodide ([DMIM]I), 1-butyl-3-methylimidazolium iodide ([BMIM]I), 1-hexyl-3-methylimidazolium iodide ([HMIM]I), 1-hexyl-3-methylimidazolium chloride ([HMIM]Cl), and 1-methyl-3-octylimidazolium chloride ([MOIM]Cl). Immediately after photoexcitation, an induced absorption was observed at various probe wavelengths (555−1556 nm). Afterward, the decay of the induced absorption was found to be independent of the alkyl chain length and viscosity of the ionic liquids. Two alternative mechanisms were proposed to explain the dynamics. In a first scenario excess electrons are generated through one-photon photodetachment of halides analogous to aqueous halide photodetachment. The dynamics in this case were analyzed with the help of a competing kinetic model proposed for geminate recombination in aqueous chloride photodetachment. Alternatively, imidazolium cations may be subject to photoionization. The transient NIR absorption can then be assigned to imidazolium dimer radical cations and/or excess electrons which may be formed upon association of imidazolium radicals with their parent cations. Both scenarios suggest that a thorough explanation of the ultrafast dynamics probably requires the implication of cooperative effects in the ionic liquids upon photoexcitation.

1. Introduction

Room temperature ionic liquids (RTILs) have attracted tremendous attention in the past few years due to their unique properties such as low vapor pressure, high thermal and chemical stability, and inflammability and their strong potential to replace conventional volatile organic solvents in many chemical and industrial applications.[1−8] Several special issues have been devoted to "Physical Chemistry of Ionic Liquids", especially their intermolecular interactions, solvation dynamics, and electrochemistry (see e.g., *J. Phys. Chem. B* **2007**, special issue 18, and ref 9). More importantly, RTILs based on the imidazolium cation have recently been used as electrolytes in dye-sensitized solar cells.[10−16] In light of the importance of RTILs in many applications, a comprehensive understanding of their photochemistry and the dynamics of charge transfer and charge recombination is mandatory. Although time-resolved dynamics of RTILs during photolysis and pulse radiolysis have been reported in a number of recent studies,[17−25] the detailed photochemistry of RTILs and product distribution is only poorly understood. It was shown that solvated electrons were the main radiolysis product formed in ammonium cation based RTILs under pulse radiolysis conditions.[18,19] We reported for the first time that solvated electrons can also be generated by direct femtosecond UV photolysis of various RTILs.[20−22] Furthermore, the decay of solvated electrons strongly depends on the counteranion from which the electrons are generated. For example, in the case of pure RTILs based on phosphonium (e.g., $[R_4P]$) or pyrrolidinium cations (e.g., [BMPyrr]) with bis(trifluoromethylsulfonyl)imide, $[NTf_2]$, as a counteranion solvated electrons were found to have long lifetimes of at least hundreds of picoseconds (ps).[20] However, when 1-butyl-1-methylpyrrolidinium bis(trifluoromethylsulfonyl)imide, $[BMPyrr][NTf_2]$, is doped either with 1,1-dimethylpyrrolidinium iodide or tetrabutylammonium iodide (TBAI), the majority of these excess electrons undergo fast decay through recombination.[22] On the other hand, Shkrob et al.[26] have shown that solvated electrons generated through pulse radiolysis and UV photolysis are rapidly captured by imidazolium cations. The aim of the present study is to investigate in more detail the ultrafast processes after one-photon photodetachment of imidazolium cation based RTILs containing halides as anions. In addition, the influence of temperature and viscosity on the recombination dynamics will be tested. Therefore, RTILs are chosen with increasing length of alkyl chains attached to the cation (longer chain length results in higher viscosity). Such information may be of great help in designing suitable ionic liquids that can be employed in photoinduced applications.

2. Experimental Section

A complete description of our laser systems employed in this study, the sample preparation, and the pump−probe measurements can be found elsewhere.[22,27,28] Briefly, one of the systems was a fully integrated 1 kHz femtosecond laser system (Clark-MXR, CPA 2210) with a central wavelength of 775 nm and a pulse duration of 200 fs. One part of the output was frequency-doubled in a BBO to pump a commercial NOPA system according to the design published in ref 29 capable of delivering probe pulses from the visible to the NIR region. UV pump pulses ($\lambda = 257$ nm, intensity $\sim 10^8$ W/cm^2 at time resolution $\sim$150 fs) were obtained by third harmonic generation of another portion of the RGA output. In the pump−probe absorption studies the change of the optical density was monitored with and without pump pulse (ΔOD) as a function of delay time. Positive ΔOD values correspond to pump-induced absorption. All measurements were carried out under nonfocused conditions of the pump pulse to avoid nonlinearities in the quartz cuvette.

* Corresponding author. E-mail: andreas.unterreiner@kit.edu.

10.1021/jp804861z CCC: $40.75
Published on Web 11/12/2008

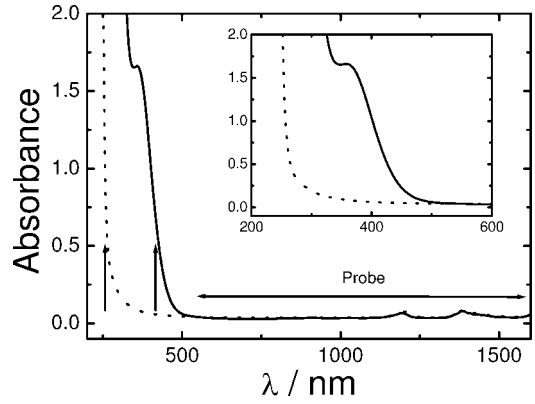

Figure 1. Static absorption spectra of RTILs [HMIM]Cl (dotted line) and [BMIM]I (solid line). Pump (257 nm) and probe wavelength region are indicated by arrows.

Reference measurements in these cuvettes without RTILs gave no transient response under these conditions. Our second laser system consisted of a home-built Ti:sapphire femtosecond laser oscillator and a regenerative amplifier (RGA) operating at 800 nm. The excitation wavelength at 400 nm was obtained by frequency doubling a fraction of the main output in a BBO crystal. Probe wavelengths ranging from 555 to 1556 nm were obtained with the help of a home-built NOPA system.

The ionic liquids, 1,3-dimethylimidazolium iodide [DMIM]I, 1-butyl-3-methylimidazolium iodide [BMIM]I, 1-hexyl-3-methylimidazolium halide [HMIM]X (X = Cl, I), and 1-methyl-3-octylimidazolium chloride [MOIM]Cl, were purchased from Merck/EMD in the highest quality available (purity >99%) and were used without any further purification. As shown previously,[22] effects of small water content (~100 ppm) and other impurities occur on time scales of >100 ps. The liquids were filled in 1 mm cuvettes in an argon box to avoid any air contamination. Exemplary UV−vis absorption spectra are shown in Figure 1 for [HMIM]Cl and [BMIM]I where the pump and probe wavelengths are also indicated (vertical and horizontal arrows, respectively).

3. Results

3.1. 1-Alkyl-3-methylimidazolium Iodides. The transient response of pure [DMIM]I after excitation with a 257 nm pulse is shown in Figure 2a. The transient profiles observed at various probe wavelengths beyond 1200 nm are identical. The induced absorption undergoes a rapid decay within the first few picoseconds. It was shown in previous studies[22] that during photolysis di- and triiodides are generated along with excess charges, and the contribution of such species to the induced absorption is shown to be considerable only at shorter probe wavelengths. These species have been found to have absorption bands peaking at 335 and 750 nm in various polar solvents such as ethanol and acetonitrile.[30,31] A closer look of the transient absorption profiles indicate that ~90% of the induced absorption decays within a few picoseconds, while at probe wavelengths around 1200 nm the residual absorption undergoes a very slow decay over hundreds of picoseconds.

Pump induced absorption profiles in neat [BMIM]I and [HMIM]I are shown in Figures 2b and 2c, respectively. The nature and dynamics of the absorption profiles appear similar to those observed in [DMIM]I. The probable interference of di- and trihalides with the dynamics of induced absorption at $\lambda_{probe} \leq 1200$ nm is demonstrated in Figure 3 where transient profiles are shown for probe wavelengths 1200 and 1400 nm

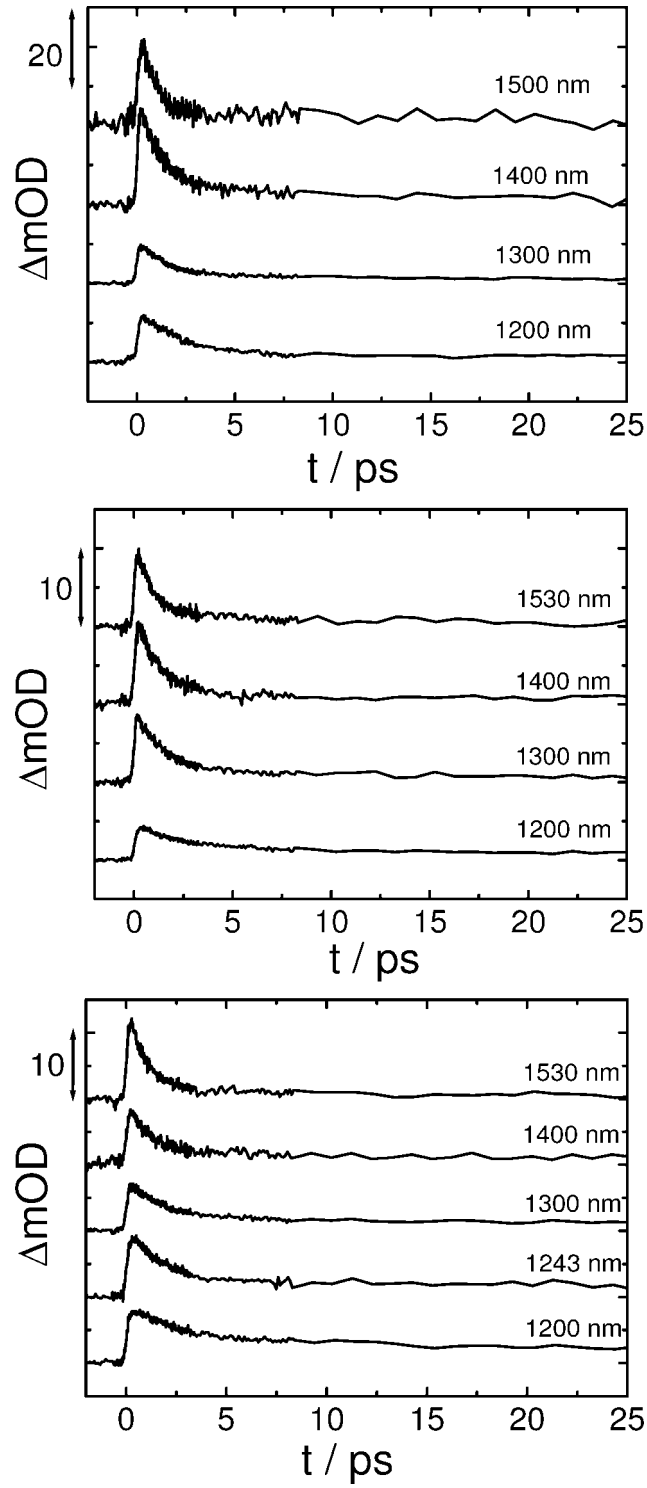

Figure 2. Time-resolved induced absorption at multiple probe wavelengths in (a) [DMIM]I, (b) [BMIM]I, and (c) [HMIM]I.

in [HMIM]I. It can be clearly seen that within the first few picoseconds a large fraction of the induced absorption decays at wavelengths ≥1200 nm. The reason for the behavior of the induced absorption profile at 1200 nm may be the contribution from long-lived di- and triiodides as shown in our previous study[22] (see also sections 4.2.1 and 4.2.2). In fact, the tail of the low-energy absorption band of I_2^- in ethylene glycol peaking at 750 nm was found to extend up to almost 1200 nm.[32]

3.2. 1-Alkyl-3-methylimidazolium Chlorides. Induced absorption profiles recorded after 257 nm photolysis of [HMIM]Cl and [MOIM]Cl at a probe wavelength of 1530 nm are shown

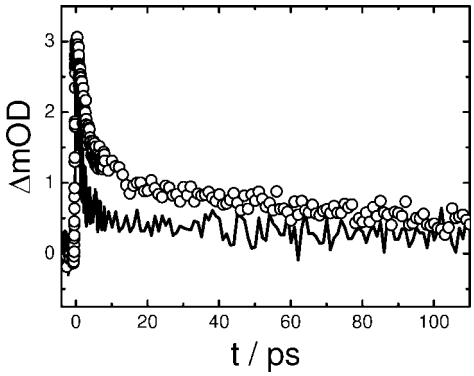

Figure 3. Comparison of the induced absorption in [HMIM]I at 1200 (circles) and 1400 nm (solid line).

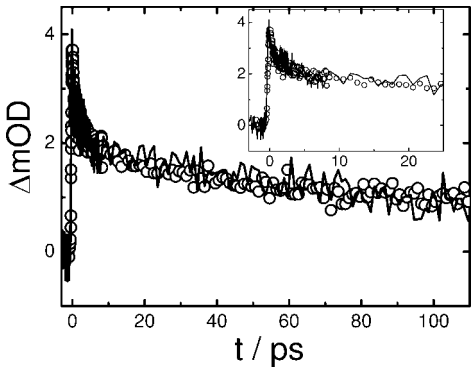

Figure 4. Time-resolved induced absorption in [HMIM]Cl (circles) and [MOIM]Cl (solid line) at a probe wavelength of 1530 nm.

in Figure 4. As can be seen, the nature of the induced absorption is similar in [HMIM]Cl and [MOIM]Cl. Furthermore, the only difference between iodides and chlorides is the fraction of the induced absorption undergoing decay. For example, in the case of imidazolium iodides the ΔOD amplitude decreases by more than 90% within the first few picoseconds, whereas nearly ~40% of the initial absorption in chlorides can be observed after 100 ps. The differences in the dynamics of the induced absorption in chlorides and iodides are discussed in more details in section 4. Despite a relatively higher viscosity of [MOIM]Cl compared to that of [HMIM]Cl, the dynamics are identical in both RTILs as was observed with imidazolium iodides. The viscosities of [HMIM]Cl and [MOIM]Cl were reported to be ~18 000 and ~21 000 cP, respectively.[33]

3.3. Temperature-Dependent Studies. Pump-induced transients are recorded in various RTILs at temperatures between 298 and 373 K to investigate the behavior of the dynamics at elevated temperatures. Parts a and b of Figure 5 display induced absorption in [HMIM]I and [HMIM]Cl, respectively, at a probe wavelength of 1530 nm at various temperatures. The induced absorption profiles are comparable at all temperatures within the signal-to-noise ratio (about 10:1). Similar results were obtained in all other RTILs investigated in this study. It is obvious from these observations that the dynamics are insensitive to a temperature change although the viscosity decreases strongly with a rise in temperature.[34]

4. Discussion

4.1. Effect of Alkyl Chain Length and Temperature on the Dynamics. A closer examination of Figure 2a−c suggests that the room temperature dynamics of the pump induced absorption in imidazolium iodides are independent of the viscosity of the medium because the latter is reported to depend

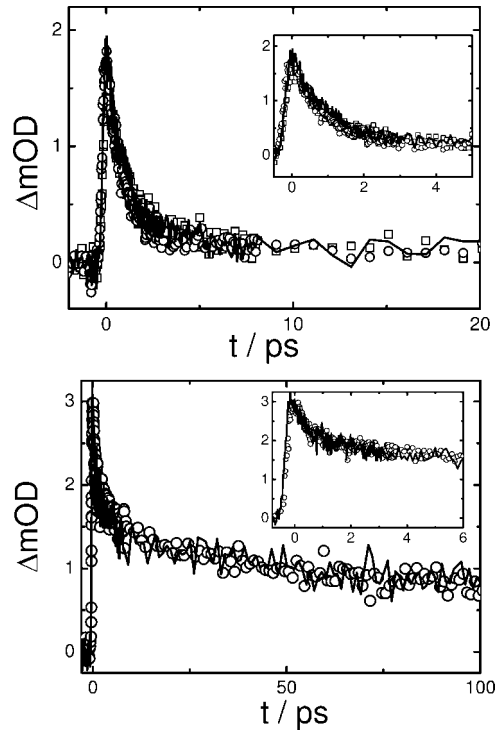

Figure 5. Effect of temperature on the ultrafast response at a probe wavelength of 1530 nm in (a) [HMIM]Cl (circles: RT; solid line: 60 °C; squares: 100 °C) and (b) [HMIM] (circles: RT; solid line: 120 °C).

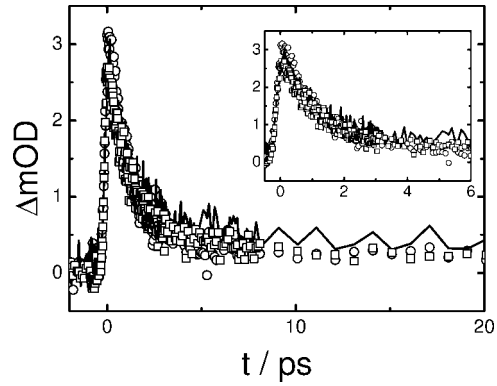

Figure 6. Time-resolved induced absorption at a probe wavelength of 1400 nm in [DMIM]I (circles), [BMIM]I (solid line), and [HMIM]I (squares). Influence of chain length on the ultrafast dynamics.

strongly on the alkyl chain length.[35−37] This is exemplarily demonstrated in Figure 6 where the induced absorption profiles are shown at a probe wavelength of 1400 nm for [DMIM]I, [BMIM]I, and [HMIM]I. To give more quantitative values, the viscosity was reported to increase from ~1000 to 3400 cP when a propyl group was replaced by a nonyl group in 1-alkyl-3-methylimidazolium iodide.[10] This suggests that the mobility of transients in RTILs should decrease with increasing length of the carbon chain and thereby with increasing viscosity, hence affecting the recombination dynamics as was reported in many polar and nonpolar solvents.[38−40] However, the dynamics in the present investigation are not sensitive to the changes in the viscosity of RTILs and behave differently from low viscous polar and nonpolar liquids.

The pump induced absorption and its subsequent decay shown in Figure 5a for [HMIM]I for a probe wavelength of 1530 nm are almost identical at various temperatures. These results clearly demonstrate that changes of the temperature and thus viscosity

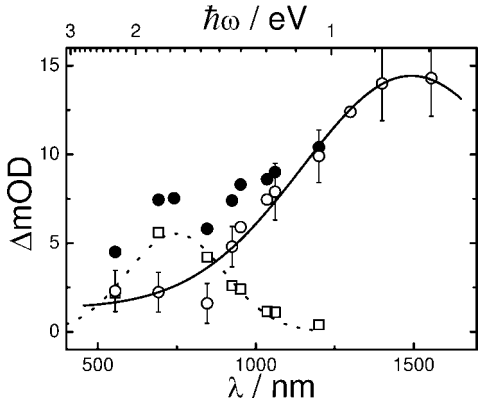

Figure 7. Transient absorption spectrum of excess electrons in [BMIM]I after 400 nm excitation (see text for full explanation of the symbols).

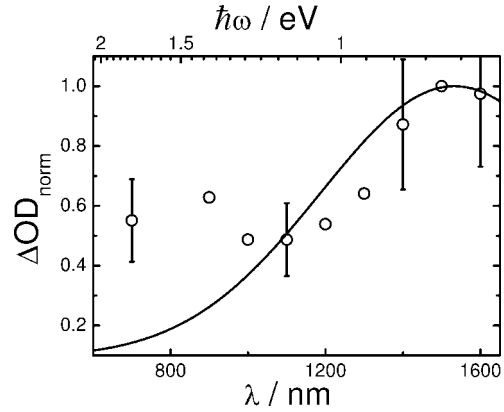

Figure 8. Raw transient absorption spectrum of excess electrons taken at a delay of 10 ps in [HMIM]Cl after excitation at 257 nm. The solid line represents the Gaussian fit obtained for [BMIM]I for comparison.

SCHEME 1: Generation of Excess Electrons after One-Photon Photolysis of Imidazolium Halides

$$X^- + \hbar\omega_{laser} \longrightarrow (X^-)^*_{CTTS} \xrightarrow{k_p} (X:e^-) \xrightarrow{k_d} e^-_{solv} + X$$
$$\downarrow k_{nr} \qquad\qquad \downarrow k_n \qquad\quad \downarrow k_r$$
$$X^- \qquad\quad X^- \text{and/or [Im]} \qquad P$$

of the system do not affect the dynamics on a picoseconds time scale. It is interesting to note that the fast relaxation dynamics on a picoseconds time scale in various pyrrolidinium-based ionic liquids investigated with the femtosecond optical heterodyne-detected Raman-induced Kerr effect spectroscopy (OHD-RIKES) technique were found to be independent of viscosity, while the slower dynamics on the nanosecond time scale scale with the viscosity of the medium,[41] strongly suggesting that ultrafast dynamics in RTILs behave differently than in other polar/nonpolar liquid media.

4.2. Generation of Transient Species Absorbing in NIR Region. Before we discuss the dynamics of the induced absorption, it is important to consider various photolysis processes that contribute to the induced absorption, especially in the near-IR probe wavelength domain. Here we consider two scenarios where photoexcitation of anions and cations leads to the generation of *electron:halogen* pairs and/or imidazolium dimer cation radicals. However, as we will see later, unambiguous assignment of the transient NIR absorption to either of these transients is not possible in the present investigation.

4.2.1. Scenario I. The immediate rise of the absorbance indicates the formation of a new transient species. Supposing this would be an excess charge generated via CTTS excitation of halides, the excess energy would be low (red-edge excitation) and its mobility reduced. Consequently, the electron is likely to reside close to the parent halogen. The subsequent decay of the transient absorbance within roughly 2 ps at all wavelengths suggests fast recombination steps. Because of the low kinetic excess energy of the charge, it is unlikely that this species corresponds to a fully solvated electron immediately after photoexcitation. On the other hand, it may very well be that halogen:electron pairs are formed. This assumption is further supported by the observation that variation of chain length and temperature does not influence the ultrafast dynamics significantly. Especially, the independence on chain length is indicative that the excess charge must be located near the cation center (imidazolium) and not the alkyl side chains. Consequently, the dynamics may be analyzed with a modified kinetic model (Scheme 1) originally developed by Staib and Borgis for halide photodetachment in aqueous medium,[42,43] where k_p, k_d, and k_n describe the fast formation of [X:e$^-$] pairs (k_p), its dissociation into fully solvated electron and a halogen atom (k_d), and the reaction of excess electrons with iodine atoms and/or imidazolium cations (k_n), respectively. k_{nr} is the nonradiative deactivation rate of $(X^*)_{CTTS}$. Possible side reactions under our experimental conditions are di- and trihalide formation (<1200 nm)

$$X + X^- \rightarrow X_2^- \tag{S1}$$

$$2X_2^- \rightarrow X_3^- + X^- \tag{S2}$$

Neta and co-workers[44] have demonstrated that excess electrons generated by pulse radiolysis of various imidazolium-based RTILs are efficiently scavenged by imidazolium cations. Such reduced radicals have very narrow absorption spectra peaking around 350 nm with an approximate full half-width (fhwm) of 0.35 eV.[19] Generation of imidazolium radicals upon reduction was also demonstrated by Shkrob et al. with the help of EPR spectroscopy.[26] Our experimental setup does not allow tuning of probe wavelengths below 550 nm and hence limits the observation of reduced radicals in the UV region. Therefore, the rate constant k_n cannot be assigned to a specific recombination process; i.e., excess electrons either react with halogen atoms within the electron:halogen pair or they are captured by imidazolium cations. The reaction of solvated electrons with imidazolium cations was also found to be very efficient with a bimolecular rate constant of 2×10^{10} L mol^{-1} s^{-1}.[44] From this mechanism one can deduce the following expression:[42]

$$\Omega(t) = \frac{k_d}{k_d + k_n} + \frac{k_p}{k_d + k_n - k_p}\left[\frac{k_p - k_d}{k_p}\exp\{-k_p t\} - \frac{k_n}{k_n + k_d}\exp\{-(k_d + k_n)t\}\right] \tag{1}$$

Here, the quantity $\Omega(t)$ represents simply the experimentally obtained $\Delta OD(t)$ values. We have analyzed the pump induced absorption profiles in imidazolium halides using eq 1. The fits seem to describe the rise and the decay kinetics reasonably well for multiple probe wavelengths as can be seen in Figure 9a, where an exemplary fit (gray curve) is shown for the transient response in [BMIM]I at a probe wavelength of 1400 nm. The average time constants obtained from such an analysis for the three processes are $1/k_p \sim 110$ fs, $1/k_n \sim 2$ ps, and $1/k_d \sim 25$

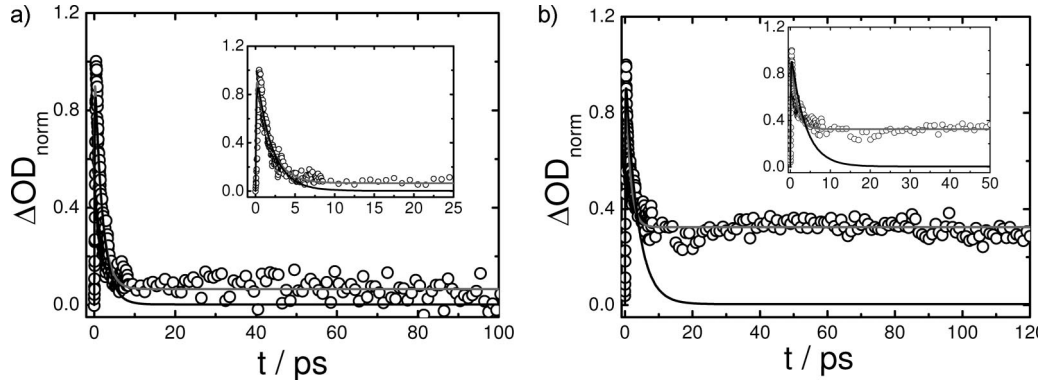

Figure 9. Analysis of the ultrafast response using eq 1 in (a) [BMIM]I and (b) [HMIM]Cl. Black curve is fitted taking the $1/k_d$ value for iodide photodetachment in pure ethylene glycol (~850 ps) from ref 45.

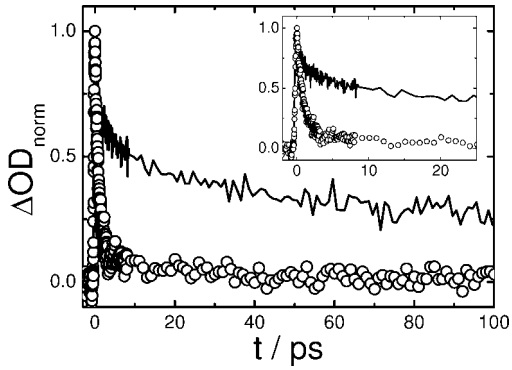

Figure 10. Comparison of ultrafast response in [HMIM]I (circles) and [HMIM]Cl (solid line) at a probe wavelength of 1530 nm.

ps. Application of this model to chloride photodetachment yields $1/k_p \sim 110$ fs, $1/k_n \sim 5$ ps, and $1/k_d \sim 11$ ps. The results suggest that excess electrons undergo fast and efficient recombination ($1/k_n \sim 2$ ps), leading to very low escape yields in imidazolium iodides. However, much higher escape yields (~40%) are observed in the chloride system (see Figures 9b and 10). The higher escape yields are also reflected in faster dissociation rates of [Cl:e^-] pairs compared to [I:e^-] pairs (see section 4.3 for more details).

Assuming that the dissociation of contact pairs ($1/k_d$) is diffusion controlled and taking the value determined by Bradforth and co-workers[45] for $1/k_d$ in the iodide photodetachment in pure ethylene glycol, eq 1 fails to describe the decay of the induced absorption satisfactorily (see Figure 9a, black curve). This disparity is more clearly demonstrated in the case of chloride photodetachment in Figure 9b. These observations imply that the escape process of excess electrons from contact pairs in RTILs is not diffusion controlled in contrast to various polar solvents. The faster dissociation of the contact pair in high viscous imidazolium halides may be explained with the help of tunneling process. We, therefore, propose that excess electrons in contact pairs generated in the photodetachment of halides in RTILs tunnel through the free energy barrier of these contact pairs. Using simple quantum mechanical calculations,[46] the probability and tunneling rate for the excess electron can be estimated. In the following, a one-dimensional box potential is used as already considered for HTILs.[47] The length of the box is set to 12 Å, i.e., the mean distance between two imidazolium cations and the barrier itself to 6 Å. The latter value is reasonable on the basis of the center of mass separation of the contact pairs.[42,45] If the barrier height is assumed to be 1 eV, the 1/e time of the tunneling process turns out to be ~6 ps. Considering the simplicity of the model and various other factors which may influence the tunneling rate (e.g., free charges of both cations and anions), this is in good agreement with the time constant for the dissociation of chlorine:electron pairs of 11 ps.

SCHEME 2: Generation of Excess Electrons in One-Photon Photolysis of Imidazolium Halides

Excess charge generation:	$C^+ \xrightarrow{h\nu} C^{2+} + e^-$	(2)
Reduction of dication radicals:	$C^{2+} + X^- (\text{or } e^-) \rightarrow C^{+*} + X$	(3)
Electron:halogen contact pairs:	$\overline{C^+ + X^- \xrightarrow{h\nu} C^{+*} + (X:e^-)}$	(4)
Dimer formation:	$C^+ + C^{+*} + X^- \leftrightarrow C_2^+ + X$	(5)

4.2.2. Scenario II. Alternative to scenario I, the transient absorption in the NIR region may be equally attributed to the imidazolium dimer radicals generated as shown in Scheme 2. As stated above, the reduced/oxidized imidazolium radials may not absorb in this region when isolated. However, it is possible that such radicals associate with the parent imidazolium cations forming dimer radical cations.

As considered in Scheme 2, imidazolium cations undergo photoinduced electron transfer upon photoexcitation generating dications (reaction 2). The excitation energies employed in this investigation are too low to ionize imidazolium cations directly to give excess charges. Instead, reaction 2 can be possible due to the stabilization of imidazolium cations by reaction 3. As a result, dications are rapidly reduced by an electron transfer from a nearby anion as shown by Shkrob et al.[26] (reaction 3) or by directly capturing the excess electron generated in reaction 4.[44] Similar to the reaction 1 in Scheme 1, electron:halogen contact pairs are generated indirectly in reaction 4 through cation ionization. Such pairs are indistinguishable in both the scenarios. The imidazolium trapped-electron radicals formed in reaction 3 may associate immediately with the parent imidazolium cations through a three-electron C−C bond leading to the formation of dimer radical cations (reaction 5). Analogous processes are known to occur in the γ-radiolysis of acetonitrile at 77 K, leading to the formation of dimer radical anions.[48] Aromatic dimer radicals are reported to have broad absorption bands in the NIR region[49−51] but are not yet known for ionic liquids. Ito and co-workers[49] have shown that transient species with two broad absorption bands at 590 and 1100 nm were generated on UV-laser excitation of naphthylalkanes. The absorption band at 1100 nm was assigned to a charge resonance (CR) band of the intermolecular dimer radical cations of 2-ethylnaphthalene. Similarly, the absorption bands at 930 and 1030 nm were assigned to benzene dimer radicals in the γ-radiolysis of benzene at 77 K.[50]

4.3. Comparison of Scenarios I and II. ***4.3.1. Transient Spectra.*** In order to be on a more sound base, transient spectra were retrieved for [BMIM]I after 400 nm excitation (Figure 7). Filled circles represent the total spectrum taken 400 fs after the excitation pulse, whereas the spectrum represented by squares is taken at 10 ps delay time. It is clear from the figure that the spectrum represented by empty circles (difference of spectra at 400 fs and 10 ps) is very broad with an fwhm of >1 eV and peaks around 1500 nm. Such broad and featureless spectra are typical for solvated electrons in high viscous liquid media such as ethylene glycol and glycerol although in the latter case the absorption maxima appear in the visible region. From theoretical calculations[42] we also know that the absorption spectrum of fully solvated electrons (e^-_{solv}) and electron:halogen pairs are supposed to be indistinguishable. If so, the transient spectra in Figure 7 should be assigned to contact pairs because it is quite unlikely to observe e^-_{solv} at 10 ps delay time (in agreement with Scheme 1).

Analogous spectra can also be retrieved from the absorption profiles of [HMIM]Cl after 257 nm excitation (see Figure 8). The raw transient absorption spectrum peaks around 800 and 1500 nm. While the 800 nm peak is most likely due to side reactions S1 and S2 (the same holds for Figure 7), the main peak at 1500 nm resembles very much that observed in Figure 7 in the iodide case.

It is noteworthy to emphasize that in both cases the formation mechanism of such contact pairs/solvated electrons is not clear. In analogy to CTTS bands in water,[52] it is indeed expected that in RTILs the corresponding CTTS bands of chlorides are blue-shifted relative to the iodide CTTS bands. For [BMIM]I, there is an intense absorption band around 380 nm (see Figure 1). The source of this band is not understood in detail. Usually, CTTS transitions of iodides in liquids occur blue-shifted by more than 1 eV relative to this band. Instead, the 380 nm band may be associated with cation absorption facilitated by a cooperative effect of cation−anion interaction in ionic liquids that may even be supported by impurities. It is important to state that the imidazolium halides were purchased in the highest quality available and used without further purification. On the other hand, it may be possible that the low-energy tails of halide CTTS bands show extended red shifts that are masked underneath the cation band. Such a scenario would be in analogy to the photoionization of neat water at energies much lower than the detachment energy expected from gas phase experiments (Urbach tail).[53] Therefore, one has to conclude that at present it is unclear how excess charges are generated under our experimental conditions.

On the other hand, the transient spectra shown in Figures 7 and 8 appear similar in nature to those reported by Ito and co-workers[49] for aromatic compounds. Similarly, a transient species having a broad absorption band with a peak at 920 nm and extending beyond 1000 nm were reported to be formed within 1 ps following a two-photon excitation of liquid benzene at 268 nm.[54] Such NIR bands were attributed to CR bands of localized benzene dimer cations. Dication absorption is unlikely to occur in the NIR region as, e.g., Zhu et al.[55] have shown that laser photolysis at 266 nm (∼80 mJ/pulse) of imidazolium hexafluorophosphate led to the formation of excess electrons and dications, probably via a two-photon process. While the dications exhibit absorption spectra similar to those of reduced radicals, the low-energy tail is reported to extend up to 700 nm. In earlier works[56,57] dimer radicals were mistakenly referred to as excess electrons trapped in well-defined positions in a crystalline lattice due to their broad optical absorption spectra. In line with these findings, the transient absorption shown in Figure 2 and the transient spectra in Figures 7 and 8 are then to be assigned to CR bands of imidazolium dimer radicals formed via reactions 2−5 of Scheme 2. Unfortunately, at present such species are not known in ionic liquids. Furthermore, one would have to postulate the dimerization in RTILs to occur within the pulse duration (∼100 fs) due to the immediate rise of the induced absorption at all probe wavlengths. To make things more complicated, the formation of contact pairs cannot really be excluded from Scheme 2 (reaction 4). Furthermore, if the imidazolium dimer radicals are stable as reported for naphthyl and pyridinium alkane solutions,[49,51] the nature of the species undergoing fast decay is unclear according to scenario II. Suppose that both dimer radicals and contact pairs absorb in the NIR region a discrimination with our experimental approach is hardly possible. Finally, reaction 2 would also imply a significant reduction of the excitation energy in the iodide case, suggesting again cooperative effects in RTILs that may lower the overall excitation energy.

4.3.2. Chloride vs Iodide Relaxation Dynamics. Independent of the scenarios, the residual transient absorption at long delay times is different in chlorides and iodides. An exemplary comparison is given in Figure 10 where the induced absorption at a wavelength of 1530 nm is shown for [HMIM]I and [HMIM]Cl. According to scenario I, the relatively large residual absorption in imidazolium chlorides after several tens of picoseconds can be explained by the dissociation efficiency of electron:halogen contact pairs. In classical photochemistry of aqueous solutions of chlorides, bromides, and iodides,[58] it was shown that the dissociation efficiency of an [X:e^-] pair into a fully solvated electron and a halogen atom increases in the order $I_{aq}^- < Br_{aq}^- < Cl_{aq}^-$. This is in accordance with our observation for imidazolium iodides to chlorides. In other words, the escape yield of excess electrons in RTILs increases from iodide to chloride photodetachment. Furthermore, variation of the quantum yield of solvated electrons generated from various aqueous halides[58] reflects that the quantum yields are determined by the competition of the recombination (k_n) and dissociation (k_d) reactions which are sensitive to the parent halide ion. Faster recombination rates in high viscous imidazolium halides observed in this study can be explained on the basis of tunneling of excess electrons through the potential barrier of the contact pairs.

Alternative to the generation of electron:halogen contact pairs, large residual induced absorption in the chloride system may be explained based on scenario II, namely through the formation of imidazolium dimer cation radicals. The extent of dimerization and its absorption in NIR region may strongly depend on the nature of the halide. This is analogous to scenario I where the probability of dissociation of contact pairs depends very much on the type of halide. In the iodide case either the dimer is nonabsorbing in the NIR region or the excess electrons undergo fast recombination with iodine atoms as observed in Figure 9a and reported by Bradforth and co-workers.[45] For chloride, the dimer radical may be absorbing strongly in the NIR region as the anion interferes less with the sandwich formation of dimer radicals. We have also reported in our earlier study[22] that colorless imidazolium chlorides turn yellow on exposure to laser as well as steady-state UV photolysis. This coloring of ionic liquids may be due to the formation of such stable dimer radicals which may undergo further polymerization.

5. Conclusions

Ultrafast dynamics in room temperature ionic liquids based on the imidazolium cations and halides as counterions were

investigated with femtosecond pump−probe absorption spectroscopy. The dynamics of the induced absorption in all the RTILs studied were found to be independent of the length of alkyl chain attached to the imidazolium cation as well as on the temperature of the system. Two scenarios were offered to explain the origin of the induced absorption observed immediately after the excitation pulse at multiple probe wavelengths. In one scenario one-photon photolysis of imidazolium halides at 257 nm led to the generation of excess electrons through CTTS excitation of halides. In this case the rise and decay of the induced absorption were explained by a kinetic model originally proposed for the geminate recombination of electrons with their parent halogen atoms after one-photon photodetachment of aqueous halide solutions. In the present analysis, recombination referred to the capture of excess electrons both by imidazolium cations and by halogen atoms. However, it must be clearly stated that the formation mechanism to establish a NIR absorption as seen in Figures 7 and 8 is not understood. In an alternative mechanism (scenario II), imidazolium cations were shown to undergo photoinduced electron transfer on one-photon excitation, leading to the generation of dications which in turn were effectively reduced by electron capture. Such reduced radicals immediately associate with the parent ions generating dimer radicals that may have broad absorption bands in the NIR region. Both scenarios presented in the discussion partly explain the results, but no full description of either model has been possible yet. In order to obtain a better impression of the nature of the transient species and the formation mechanism by one-photon photolysis of imidazolium halides, further studies involving a thorough characterization of lifetimes and reaction pathways of various transient species are needed as these systems are currently only poorly understood.

Acknowledgment. We thank the CFN (Center for Functional Nanostructures) located at the University of Karlsruhe (TH) and the Deutsche Forschungsgemeinschaft (UN 108/3-1) for funding as well as Prof. Dr. H. Hippler for his generous support of this work. We also thank the referee for helpful comments and suggestions.

References and Notes

(1) Welton, T. *Chem. Rev.* **1999**, *99*, 2071.
(2) Wilkes, J. S.; Zawarotko, M. J. *Chem. Commun.* **1992**, 965.
(3) Kuang, D.; Ito, S.; Wenger, B.; Klein, C.; Moser, J.-E.; Baker, R. H.; Zakeeruddin, S. M.; Grätzel, M. *J. Am. Chem. Soc.* **2006**, *128*, 4146, and references cited therein.
(4) Mazille, F.; Fei, Z.; Kuang, D.; Zhao, D.; Zakeeruddin, S. M.; Grätzel, M.; Dyson, J. P. *Inorg. Chem.* **2006**, *45*, 1585.
(5) Kawano, R.; Watanabe, M. *Chem. Commun.* **2005**, 2107.
(6) Sakaebe, H.; Matsumoto, H. *Electrochem. Commun.* **2003**, 5594, and references cited therein.
(7) Nada, A.; Susan, M. A. B. H.; Kudo, K.; Mitsushima, S.; Hayamizu, K.; Watanabe, M. *J. Phys. Chem. B* **2003**, *107*, 4024.
(8) Nanjundiah, C.; McDevitt, S. F.; Koch, V. R. *J. Electrochem. Soc.* **1997**, *144*, 3392.
(9) Castner, E. W., Jr.; Wishart, J. F.; Shirota, H. *Acc. Chem. Res.* **2007**, *40*, 1217.
(10) Kubo, W.; Kambe, S.; Nakade, S.; Kitamura, T.; Hanabusa, K.; Wada, Y.; Yanagida, S. *J. Phys. Chem. B* **2003**, *107*, 4374.
(11) Wang, P.; Zakeeruddin, S. M.; Moser, J.-E.; Grätzel, M. *J. Phys. Chem. B* **2003**, *107*, 13280.
(12) O'Regan, B.; Grätzel, M. *Nature (London)* **1991**, *353*, 737.
(13) Hagfeldt, A.; Grätzel, M. *Chem. Rev.* **1995**, *95*, 49.
(14) Hagfeldt, A.; Grätzel, M. *Acc. Chem. Res.* **2000**, *33*, 269.
(15) Grätzel, M. *Nature (London)* **2001**, *414*, 338.
(16) Yamanaka, N.; Kawano, R.; Kubo, W.; Masaki, N.; Kitamura, T.; Wada, Y.; Watanabe, M.; Yanagida, S. *J. Phys. Chem. B* **2007**, *111*, 4763.
(17) Wishart, J. F.; Lall-Ramnarian, S. I.; Raju, R.; Scumpia, A.; Bellevue, S.; Ragbir, R.; Engel, R. *Radiat. Phys. Chem.* **2005**, *72*, 99, and references cited therein.
(18) Wishart, J. F.; Neta, P. *J. Phys. Chem. B* **2003**, *107*, 7261.
(19) Behar, D.; Neta, P.; Schultheisz, C. *J. Phys. Chem. A* **2002**, *106*, 3139.
(20) Chandrasekhar, N.; Endres, F.; Unterreiner, A.-N. *Phys. Chem. Chem. Phys.* **2006**, *8*, 3192.
(21) Chandrasekhar, N.; Unterreiner, A.-N. *Z. Phys. Chem.* **2006**, *220*, 1235.
(22) Brands, H.; Chandrasekhar, N.; Unterreiner, A.-N. *J. Phys. Chem. B* **2007**, *111*, 4830.
(23) Katoh, R.; Yoshida, Y.; Katsumura, Y.; Takahashi, K. *J. Phys. Chem. B* **2007**, *111*, 4770.
(24) Takahashi, K.; Sakai, K.; Tanka, H.; Hiejima, Y.; Katsumura, Y.; Watanabe, M. *J. Phys. Chem. B* **2007**, *111*, 4807.
(25) Shirota, H.; Wishart, J. F.; Castner, E. W., Jr. *J. Phys. Chem. B* **2007**, *111*, 4819.
(26) Shkrob, I. A.; Chemerisov, S. D.; Wishart, J. F. *J. Phys. Chem. B* **2007**, *111*, 11786.
(27) Unterreiner, A.-N. Ph. D. Thesis, Universität Karlsruhe (TH), 1998, ISBN: 3-89653-368-1.
(28) Schalk, O.; Brands, H.; Balaban, T. S.; Unterreiner, A.-N. *J. Phys. Chem. A* **2008**, *112*, 1719.
(29) Piel, J.; Beutter, M.; Riedle, E. *Opt. Lett.* **2000**, *25*, 180.
(30) Gershgoren, E.; Gordon, E.; Ruhman, S. *J. Chem. Phys.* **1997**, *106*, 4806.
(31) Gershgoren, E.; Banin, U.; Ruhman, S. *J. Phys. Chem. A* **1998**, *102*, 9.
(32) Chandrasekhar, N.; Krebs, P. *J. Chem. Phys.* **2000**, *112*, 5910.
(33) Gomez, E.; Gonzalez, B.; Dominguez, A.; Tojo, E.; Tojo, J. *J. Chem. Eng. Data* **2006**, *51*, 696.
(34) Maginn, E. J. *Acc. Chem. Res.* **2007**, *40*, 1200.
(35) Every, H. A.; Bishop, A. G.; MacFarlane, D. R.; Orädd, G.; Forsyth, M. *Phys. Chem. Chem. Phys.* **2004**, *6*, 1758.
(36) Bonhote, P.; Dias, A.-P.; Papageorgiou, N.; Kalyanasundaram, K.; Grätzel, M. *Inorg. Chem.* **1996**, *35*, 1168.
(37) Tokuda, H.; Hayamizu, K.; Ishii, K.; Susan, Md. A. B. H.; Watanabe, M. *J. Phys. Chem. B* **2005**, *109*, 6103.
(38) Jay-Gerin, J.-P.; Ferradini, C. *Radiat. Phys. Chem.* **1990**, *36*, 317.
(39) Jay-Gerin, J.-P.; Ferradini, C. *J. Chem. Phys.* **1990**, *93*, 3718.
(40) Long, F. H.; Lu, H.; Eisenthal, K. B. *J. Phys. Chem.* **1995**, *99*, 7436.
(41) Shirota, H.; Funston, A. M.; Wishart, J. F.; Castner, E. W., Jr. *J. Chem. Phys.* **2005**, *122*, 184512.
(42) Staib, A.; Borgis, D. *J. Chem. Phys.* **1996**, *104*, 9027.
(43) Staib, A.; Borgis, D. *J. Chem. Phys.* **1995**, *103*, 2642.
(44) Behar, D.; Gonzalez, C.; Neta, P. *J. Phys. Chem. A* **2001**, *105*, 7607.
(45) Kloepfer, J. A.; Vilchiz, V. H.; Lenchenkov, V. A.; Germaine, A. C.; Bradforth, S. E. *J. Chem. Phys.* **2000**, *113*, 6288.
(46) MacQuarrie, D. A.; Simon, J. D. *Physical Chemistry: A Molecular Approach*; University Science Books: Mill Valley, CA, 1995.
(47) von Blanckenhagen, B.; Nattland, D.; Freyland, W. Proc. International Symposium in honour of Harald A. Øye, Feb 2−3, 1995, Trontheim, Norway, p 357.
(48) Sprague, E. D.; Takeda, K.; Williams, F. *Chem. Phys. Lett.* **1971**, *10*, 299.
(49) Fushimi, T.; Fujita, Y.; Ohkita, H.; Ito, S. *J. Photochem Photobiol. A: Chem.* **2004**, *165*, 69.
(50) Ekstrom, A. *J. Phys. Chem.* **1970**, *74*, 1705.
(51) Nagamura, T.; Kashihara, S.; Kawai, H. *Chem. Phys. Lett.* **1998**, *294*, 167.
(52) Fox, M. F.; Hayon, E. *J. Chem. Soc., Faraday Trans. 1* **1976**, *72*, 344.
(53) Goulet, T.; Bernas, A.; Ferradini, C.; Jay-Gerin, J.-P. *Chem. Phys. Lett.* **1990**, *170*, 492.
(54) Inokuchi, Y.; Naitoh, Y.; Ohashi, K.; Saitow, K.; Yoshihara, K.; Nishi, N. *Chem. Phys. Lett.* **1997**, *269*, 298.
(55) Zhu, G.; Wu, G.; Long, D.; Sha, M.; Yao, S. *Nucl. Sci. Technol.* **2007**, *18*, 16.
(56) Bonin, M. A.; Takeda, K.; Tsuji, K.; Williams, F. *Chem. Phys. Lett.* **1968**, *2*, 363.
(57) Takeda, K.; Williams, F. *Mol. Phys.* **1969**, *17*, 677.
(58) Jortner, J.; Ottolenghi, M.; Stein, G. *J. Phys. Chem.* **1964**, *68*, 247.

JP804861Z